

Origin of MeV ion irradiation-induced stress changes in SiO₂

M. L. Brongersma, E. Snoeks, T. van Dillen, and A. Polman^{a)}

FOM Institute for Atomic and Molecular Physics, Kruislaan 407, 1098 SJ Amsterdam, The Netherlands

(Received 18 June 1999; accepted for publication 21 March 2000)

The 4 MeV Xe ion irradiation of a thin thermally grown SiO₂ film on a Si substrate leads to four different effects in which each manifests itself by a characteristic change in the mechanical stress state of the film: densification, ascribed to a beam-induced structural change in the silica network; stress relaxation by radiation-enhanced plastic flow; anisotropic expansion and stress generation; and transient stress relaxation ascribed to the annealing of point defects. Using sensitive wafer-curvature measurements, *in situ* measurements of the in-plane mechanical stress were made during and after ion irradiation at various temperatures in the range from 95 to 575 K, in order to study the magnitude of these effects, the mechanism behind them, as well as their interplay. It is found that the structural transformation leads to a state with an equilibrium density that is 1.7%–3.2% higher than the initial state, depending on the irradiation temperature. Due to the constraint imposed by the substrate, this transformation causes a tensile in-plane stress in the oxide film. This stress is relaxed by plastic flow, leading to densification of the film. The anisotropic strain-generation rate decreases linearly with temperature from $(2.5 \pm 0.4) \times 10^{-17}$ cm²/ion at 95 K to $(-0.9 \pm 0.7) \times 10^{-17}$ cm²/ion at 575 K. The spectrum of irradiation-induced point defects, measured from the stress change after the ion beam was switched off, peaks below 0.23 eV and extends up to 0.80 eV. All four irradiation-induced effects can be described using a thermal spike model. © 2000 American Institute of Physics. [S0021-8979(00)00513-2]

I. INTRODUCTION

During ion irradiation of a solid, ionization events and atomic collisions occur in the near-surface region. These may give rise to three different phenomena that can induce a change in the mechanical stress of the irradiated region. First, morphology changes can take place.^{1–5} Second, radiation-induced Newtonian plastic flow may take place, in which the stress relaxes at a rate that is proportional to the magnitude of the stress.^{3–6} Third, a nonsaturating anisotropic stress generating effect may occur in which an in-plane stress builds up (perpendicular to the direction of the ion beam).^{4,5,7,8} The latter effect was originally discovered when free amorphous films showed anisotropic growth during high-energy irradiation;⁹ it has been found to occur in amorphous materials only, when irradiated with ions in the MeV energy range. In contrast, morphology changes and Newtonian plastic flow have been observed for both crystalline and amorphous materials at energies in the keV and MeV ranges.

In the past, we have shown that *in situ* measurements of the mechanical stress using a sensitive wafer-curvature measurement technique can provide detailed information on the three radiation-induced effects mentioned above.^{3–5} These measurements were made on thermally grown SiO₂ films on a Si substrate. The radiation-induced viscosity was determined as a function of irradiation temperature, and its magnitude was explained by a thermal spike model.⁶ We also measured the in-plane anisotropic strain generation rate at room temperature.^{4,5}

While our previous experiments have given general insight into the effects occurring during irradiation, several issues have remained unclear:

- (1) What is the interplay between structural transformations and viscous flow? At what stage during irradiation does densification due to the structural transformation take place?
- (2) How does the densification depend on irradiation temperature?
- (3) What is the temperature dependence of the anisotropic strain generation process?

In this article we will present stress measurements, made in the temperature range between 95 and 575 K that allow us to resolve these issues. In addition, we present transient stress measurements *after* the ion beam is switched off. From these we find a fourth irradiation-induced effect: the generation of volume-occupying point defects with an annihilation activation energy spectrum that depends on irradiation temperature. From the stress transients we derive the defect spectrum. Finally, we show that the four irradiation-induced effects in SiO₂ (densification, plastic flow, anisotropic stress generation, and point defect generation) are all thermal spike-related phenomena.

II. EXPERIMENT

Experiments were performed on 2.4- μ m-thick SiO₂ films grown by wet thermal oxidation (1100 °C) on 95- μ m-thick double-side polished Si(100) substrates. Rectangular samples (5×25 mm²) were clamped at one end to a copper block, leaving the other end free to bend. The clamp tem-

^{a)} Author to whom correspondence should be addressed; electronic mail: polman@amolf.nl

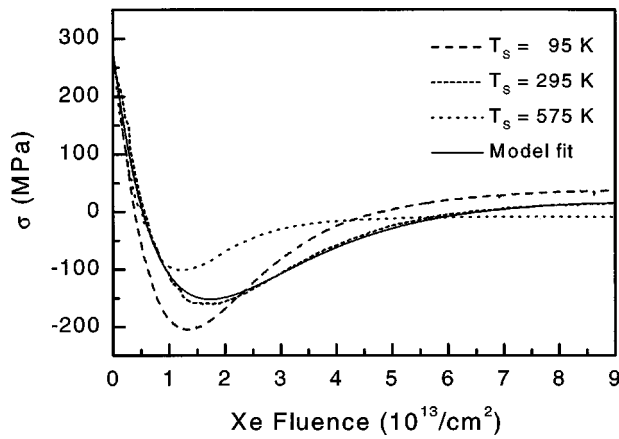


FIG. 1. *In situ* measurements of the average in-plane stress in a 2.4- μm -thick SiO_2 film on a 95- μm -thick Si(100) substrate as a function of the 4 MeV Xe fluence (dotted lines). The data were taken at 95, 295, and 575 K and each represents a set of ~ 200 data points. The solid line is a model fit of Eq. (3) to the 295 K data.

perature was kept constant in the range between 95 and 575 K by cooling with liquid N_2 or by resistively heating the copper block. Subsequently, the SiO_2 films were homogeneously irradiated by electrostatically scanning a 4.0 MeV Xe^{4+} beam over the sample at an ion flux in the range $1 \times 10^{11} - 5 \times 10^{12}$ ions/ $\text{cm}^2 \text{ s}$. Rutherford backscattering shows that the projected range of the Xe ions was 1.67 μm (well within the oxide film thickness) and that the full width at half maximum of the Gaussian Xe depth profile was 0.61 μm .

A scanning laser technique was used to *in situ* measure the radius of curvature from the back surface of the sample while it was irradiated from the front. Details of this technique are described elsewhere.¹⁰ From the radius of curvature the average in-plane stress in the SiO_2 film, σ , can be derived, using the biaxial elastic modulus of Si(100).¹¹ Local variations in film and wafer thickness limit the absolute determination of the stress to ± 6 MPa, but stress variations in a sample can be measured as accurately as 0.3 MPa. In this article, compressive stress is defined to be positive. The average in-plane strain ϵ can be calculated from the in-plane stress using the biaxial elastic modulus Y_{OX} of the oxide film: $\epsilon = \sigma / Y_{\text{OX}}$.^{12,13} In addition, ion irradiation experiments were performed on 3- μm -wide and 1- μm -deep trenches that were fabricated in a 2- μm -thick thermal oxide on a 325- μm -thick Si wafer using reactive ion etching. The distance between the trenches was 17 μm . Before and after irradiation the trenches were studied with scanning electron microscopy (SEM) using a 25 keV electron beam.

III. RESULTS AND DISCUSSION

A. Structural changes, viscous flow, and stress generation during irradiation

Figure 1 shows three measurements of the average in-plane stress σ in the SiO_2 film as a function of Xe fluence, taken at a temperature of 95, 295, and 575 K. At all these temperatures, the ion irradiation causes the initially compressive stress to turn tensile, reach a maximum tensile stress at a fluence of $(1-2) \times 10^{13}$ Xe/ cm^2 , and finally saturate. Note

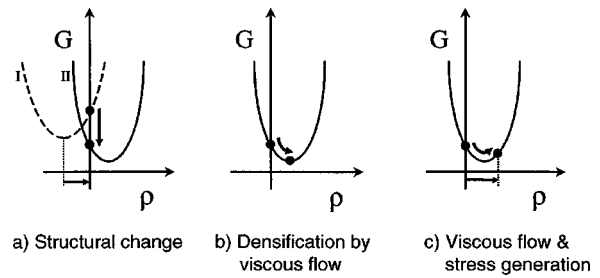


FIG. 2. Diagrams of the free energy G as a function of the density of the SiO_2 film, ρ , that schematically illustrate the following ion-irradiation induced effects: (a) effect of structural changes in the SiO_2 film, (b) densification by viscous flow, and (c) the combined effect of viscous flow and the in-plane stress generating effect. It should be noted that in practice these effects occur simultaneously.

that compressive stress is defined positive in this article. The initial compressive stress is attributed to the elastic strain caused by the difference in thermal contraction of the SiO_2 film and the Si substrate upon cooling the wafer from the oxidation temperature to the measurement temperature. We attribute the large initial stress change during ion irradiation to changes in the SiO_2 network configuration. Indeed, from optical scattering measurements it is known that ion irradiation of SiO_2 can cause changes in the network topology and O-Si-O bond angle distribution, leading to a new structural state with a higher equilibrium density.¹

Figure 2(a) schematically illustrates how such a structural change could result in a change from a compressive to a tensile stress state. The two parabolas represent the free energy, G , as a function of the density (ρ) of the SiO_2 film for two structural configurations. The parabola minima correspond to the zero strain state in each particular configuration. A deviation to the right from the zero strain state corresponds to a compressive stress state, a deviation to the left to a tensile one. The initial compressive stress state of the SiO_2 film in its initial configuration (I) is represented by the solid dot on the dashed parabola. During irradiation a new structural configuration, II, with a lower free energy minimum¹ evolves as is indicated by the solid parabola. If the density does not change, e.g., because the film is constrained by a substrate, this radiation-induced transformation to the new structural state is indicated by the vertical arrow, and leads to a tensile stress.

After the maximum tensile stress has been reached, further irradiation causes the stress to approach its saturation value after a fluence of $\approx 10^{14}$ Xe/ cm^2 . This stress change is attributed to radiation-induced plastic flow,³⁻⁶ which serves to relieve stress in the material. Note that this stress relaxation is accompanied by an increase in the density. The process of densification by viscous flow is illustrated pictorially in Fig. 2(b).¹⁴

The fact that some stress measurements in Fig. 1 saturate at a nonzero value for high-fluence irradiation indicates the presence of a continuous in-plane stress generating process.^{4,5} The nonzero saturation stress results from a dynamic equilibrium between this stress generating effect and viscous flow that serves to relax the stress. The effect of

viscous flow and the stress generating effect is depicted in Fig. 2(c).

The stress behavior as a function of fluence, φ , due to the combined effects of structural changes, plastic flow, and the anisotropic stress generating effect, can be described by the following differential equation:

$$\frac{d\sigma}{d\varphi} = Y_{\text{OX}} \left(-\frac{d\epsilon_s}{d\varphi} - \frac{\sigma}{6\eta_{\text{RAD}}} + A \right) \quad (1)$$

in which ϵ_s is the average local in-plane strain due to changes in the network structure. In the following it is assumed that the structural transformation can be described by a damage overlap model¹⁵ in which ϵ_s changes exponentially from its initial in-plane strain state, ϵ_I , to its final in-plane strain state, ϵ_{II} , after irradiation

$$\epsilon_s(\varphi) = \epsilon_I - (\epsilon_I - \epsilon_{II}) \left[1 - \exp\left(-\frac{\varphi}{\varphi_s}\right) \right] \quad (2)$$

with φ_s the typical fluence required for the structural change from state I to II. Using this assumption the solution of Eq. (1) is

$$\sigma(\varphi) = Y_{\text{OX}} \left[(-\epsilon_I + \epsilon_{\text{SAT}} - C) \exp\left(-\frac{Y_{\text{OX}}\varphi}{6\eta_{\text{RAD}}}\right) + C \exp\left(-\frac{\varphi}{\varphi_s}\right) - \epsilon_{\text{SAT}} \right] \quad (3)$$

in which $C = 6\eta_{\text{RAD}}(\epsilon_{II} - \epsilon_I)/(6\eta_{\text{RAD}} - Y_{\text{OX}}\varphi_s)$ and $\epsilon_{\text{SAT}} = -6A\eta_{\text{RAD}}/Y_{\text{OX}}$, the high-fluence saturation strain. The drawn line in Fig. 1 is the best fit of Eq. (3) to the 295 K data. The fit matches the data quite closely, indicating that an exponential strain evolution model as in Eq. (2) describes the structural transformation quite well. Slightly better fit results are achieved by separately fitting the low-fluence ($\phi < 3 \times 10^{13}$ Xe/cm²) and high-fluence ($\phi > 3 \times 10^{13}$ Xe/cm²) data. The low-fluence fits will yield more accurate values for ϵ_{II} and φ_s as the structural transformations take place during low-fluence irradiation. The high-fluence fit will give more accurate values for η_{RAD} and A , which are characteristics of structure II. Using this fit procedure for the 295 K data in Fig. 1, we find that $\varphi_s = (1.40 \pm 0.15) \times 10^{13}$ Xe/cm², $\eta_{\text{RAD}} = (2.9 \pm 0.6) \times 10^{23}$ Pa ion/cm², and $A = (1.2 \pm 0.4) \times 10^{-17}$ cm²/ion.

From this fitting procedure we also find that at 295 K $\epsilon_I = (-0.26 \pm 0.01)\%$ and $\epsilon_{II} = (0.7 \pm 0.1)\%$. It follows that the relative difference in equilibrium density (i.e., in the unconstrained state) of structures I and II $(\rho_{II} - \rho_I)/\rho_I = -3(\epsilon_{II} - \epsilon_I) = (2.9 \pm 0.3)\%$, in agreement with typical values for the density change obtained from refractive index measurements for irradiation of bulk SiO₂ glasses.^{1,2} Note that the structural transformation model in Fig. 2(a) assumes that the transformation itself does not involve a density change. Indeed, this assumption appears justified by the fact that the amount of densification obtained from our measurements using this model agrees well with values reported in the literature.

Figure 1 shows that the stress measurements taken at 95, 295, and 575 K exhibit qualitatively similar behavior and each curve can be described by Eq. (3). The temperature

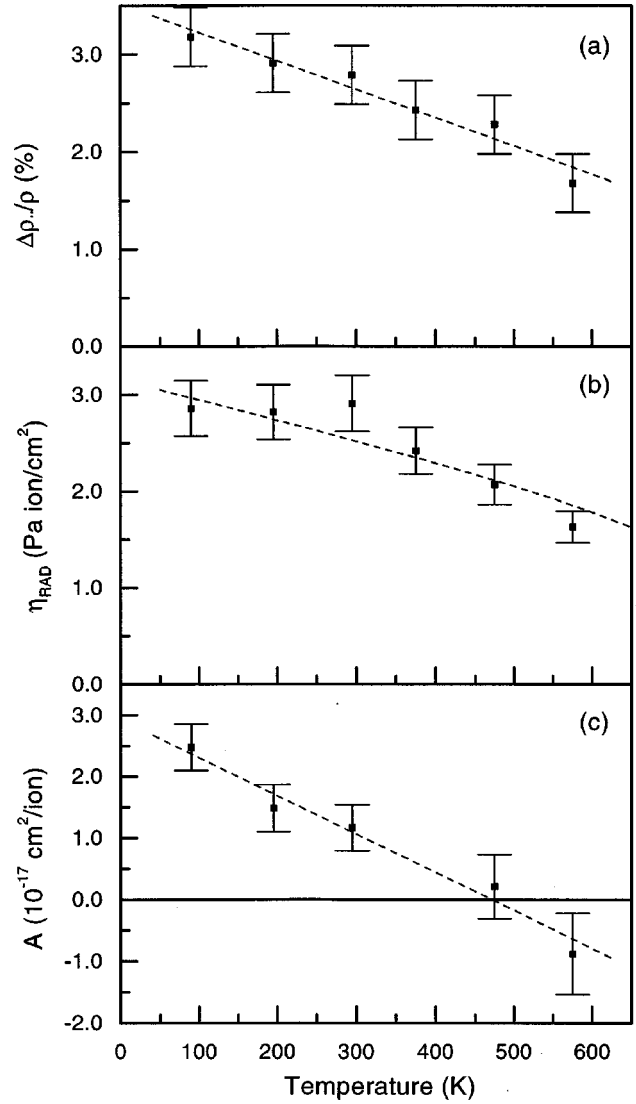


FIG. 3. Parameters describing three radiation-induced effects in silica as a function of sample temperature, obtained by fitting Eq. (3) to the data in Fig. 1: (a) relative change in equilibrium density, (b) radiation-induced viscosity, (c) in-plane stress generation rate.

dependent values of $(\rho_{II} - \rho_I)/\rho_I$, η_{RAD} , and A obtained by fitting Eq. (3) to these curves are plotted in Fig. 3. Values obtained at other temperatures not shown in Fig. 1 are included as well.

Figure 3(a) shows that the equilibrium density change decreases from 3.2% to 1.7% for irradiation temperatures increasing from 95 to 575 K. Extrapolating the data to high irradiation temperature, no densification is expected for $T > 900$ K. This is plausible since at high temperatures the glass is nearer to its equilibrium (as-grown) structure and ion irradiation will not lead to a large structural change.

Figure 3(b) shows the radiation-induced viscosity as a function of sample temperature. It is approximately constant at a value of $\eta_{\text{RAD}} = (2.9 \pm 0.3) \times 10^{23}$ Pa ion/cm² between 95 and 295 K and decreases at higher temperatures. In a separate publication the radiation-induced flow was discussed in terms of a thermal spike model,⁶ in which macroscopic stress relaxation is caused by viscous flow in hot regions of mesoscopic dimensions resulting from the energy deposition of

individual Xe ions. This model correctly predicts the magnitude and the temperature dependence of the radiation-induced viscosity [dashed line in Fig. 3(b)]. Since the densification of the SiO₂ film as described above occurs through viscous flow, the densification process can also be described in terms of a thermal spike model.

Figure 3(c) shows the anisotropic stress generation rate (A) as a function of sample temperature. It decreases roughly linearly from $(2.5 \pm 0.4) \times 10^{-17} \text{ cm}^2/\text{ion}$ at 95 K to $(-0.9 \pm 0.7) \times 10^{-17} \text{ cm}^2/\text{ion}$ at 575 K. It is interesting to compare this observation with measurements on bulk silica glasses that were irradiated with 360 MeV Xe ions. In those experiments anisotropic growth of the irradiated samples was observed, and this effect also decreased with temperature.⁸ This suggests that the anisotropic growths for 4 and 360 MeV Xe irradiation share a common origin. The anisotropic stress generation process can be described by a thermal spike model in which it is assumed that the energy deposited by a MeV Xe ion in nuclear collisions and electronic excitations causes local melting in a cylindrically shaped region around the ion track.¹⁶ The shear stress that builds up due to thermal expansion of this heated region relaxes and the viscous shear strain increment resulting from this relaxation freezes in upon cooling. Due to the anisotropic shape of the thermal spike region, this leads to a net in-plane expansion of the oxide layer, and shrinkage in the perpendicular direction. Trinkaus and Ryazanov have derived a viscoelastic continuum model¹⁶ which yields $A = (1.16/3e)[(1+v)/(5-4v)](\alpha/\rho C)S$, with v , α , ρ , C , and S Poisson's ratio, the thermal expansion coefficient, the density, the specific heat of the irradiated film at the flow temperature, and the energy deposited per unit length by a Xe ion, respectively. Using known parameters for SiO₂,^{17,18} we find that $A = 1.4 \times 10^{-17} \text{ cm}^2/\text{ion}$, in the same range as what we find in our measurements [see Fig. 3(c)]. The decrease of A with increasing irradiation temperature may be due to the fact that at high temperature the in-plane strain that is generated by each thermal spike is partly relaxed after the thermal spike phase due to the lower thermal viscosity of the matrix glass at high temperature.^{16,19}

The ion irradiation-induced deformation of a repetitive pattern of trenches etched in a SiO₂ film is also a sensitive alternative probe for the anisotropic stress generating process.⁴ Figure 4(a) shows a SEM image of a 3- μm -wide unimplanted trench with sharply defined sidewalls. The angle of view is such that both the surface of the SiO₂ film as well as the cross section are visible. Figure 4(b) shows a trench that has been irradiated at normal incidence to the film surface with $3 \times 10^{15} \text{ Xe}/\text{cm}^2$ at 4.0 MeV at 295 K. A dramatic deformation of the trench is observed, and is attributed to the anisotropic deformation phenomenon, as discussed previously.⁴ Dividing the relative in-plane expansion of the SiO₂ surface ($\Delta l/l \approx 0.1$) by the ion fluence, the deformation rate A is estimated to be $3 \times 10^{-17} \text{ cm}^2/\text{ion}$, of the same order as the value for A at 295 K in Fig. 3(b). Figure 4(c) shows a trench after a similar irradiation ($3 \times 10^{15} \text{ Xe}/\text{cm}^2$ at 4.0 MeV) at a temperature of 575 K. Almost no deformation is observed in this case, in agreement with Fig. 3(c), showing that A is small at higher temperatures.

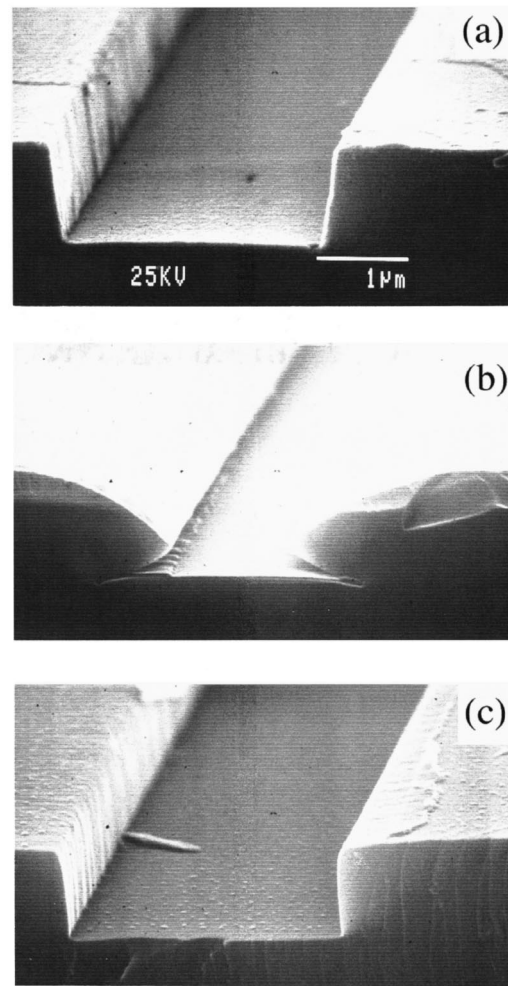


FIG. 4. Cross section SEM images of a 3.0- μm -wide trench in a 2- μm -thick thermally grown SiO₂ film on Si before irradiation (a), and after 4 MeV irradiation with $3 \times 10^{15} \text{ Xe}/\text{cm}^2$ at room temperature (b) or 575 K (c). The ion beam was directed perpendicular to the surface.

B. Transient effects after irradiation: Structural relaxation

In the following, we will describe transient measurements of the stress after the ion beam is switched off. Experiments were performed on one sample that was first irradiated at 95 K at a flux of $5 \times 10^{12} \text{ Xe}/\text{cm}^2 \text{ s}$ to a fluence sufficient to reach saturation (see Fig. 1). After equilibrium was reached, the ion irradiation was stopped and the stress was measured as a function of time. The stress change, $\Delta\sigma$, with respect to the saturation stress during irradiation is plotted in Fig. 5 as a function of time. At times shorter than roughly 1 s after the beam was switched off, no significant change in stress occurs. After that, the stress decreases roughly linearly on a logarithmic time axis, and a stress change of approximately 6 MPa is observed in the first 700 s (95 K data in Fig. 5). Note that this stress change is much smaller than the changes due to structural transformations and viscous flow during ion irradiation as seen in Fig. 1. After this measurement, the temperature was increased to 135 K, and the procedure (irradiation to equilibrium stress and measuring the stress after stopping the ion beam) was repeated. These data, along with data taken at 195 and 255

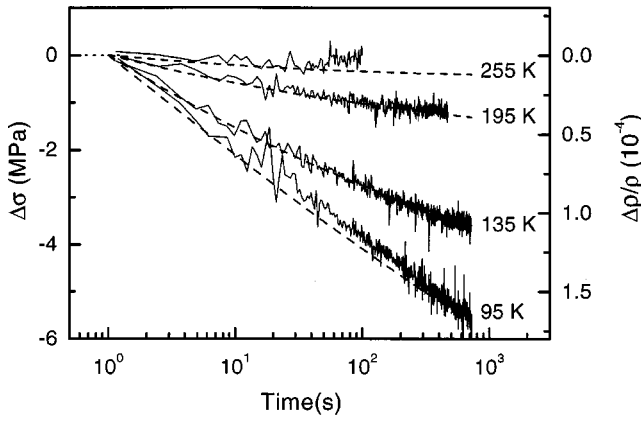


FIG. 5. The average in-plane stress change in the SiO₂ film after the 4 MeV Xe ion beam was switched off, measured with respect to the saturation stress, plotted on a logarithmic time scale. Results are shown for sample temperatures of 95, 135, 195, and 255 K. At each of these temperatures the samples were irradiated with a fluence sufficient to reach the saturation stress value. The dashed lines are calculations of the stress changes using the continuous spectrum in Fig. 6 and Eq. (4).

K, are also plotted in Fig. 5. As can be seen, the rate at which the stress changes decreases with increasing temperature and above 255 K no substantial stress changes are observed.

The negative stress changes in Fig. 5 are qualitatively similar to what has been observed after irradiation of a soda lime borosilicate glass at room temperature.^{5,20} In that case, it was shown that the stress changes were not driven by the stress itself (i.e., are not due to plastic flow), but can be attributed to relaxation to a structure with a higher equilibrium density. As the film remains constrained by the substrate, this relaxation leads to the buildup of a tensile stress. The relative change in equilibrium density (i.e., in the unconstrained state) due to this structural relaxation can be calculated from the change in the average in-plane stress by $\Delta\rho/\rho = -3\Delta\sigma/Y_{OX}$, where ρ is the density of the irradiated region before the ion beam was switched off. The relative density increase that was calculated in this way is shown on the right hand axis in Fig. 5. For example, at $T=95$ K, we find that $\Delta\rho/\rho = 1.7 \times 10^{-4}$ after the first 700 s.

Densification by structural relaxation can be described by the annealing of volume occupying point defects that have a spectrum of relaxation times. Assuming a unimolecular recombination mechanism, the time dependence of this densification is given by²¹

$$\Delta\rho(t) = \Delta\rho_\infty - \int_0^\infty D(Q) \cdot \exp[-t/\tau(Q)] dQ, \quad (4)$$

where $D(Q)$ is the density change of the film in units of atomic density per unit energy due to the annihilation of defects that exhibit a characteristic annealing time τ . This time depends on the activation energy, Q , for annihilation of the defect

$$\tau = \frac{h}{kT} \exp(Q/kT), \quad (5)$$

with k and h Boltzmann's and Planck's constants, respectively. If the activation energy spectrum is a slowly varying function of energy it can be shown that, at a time t after the

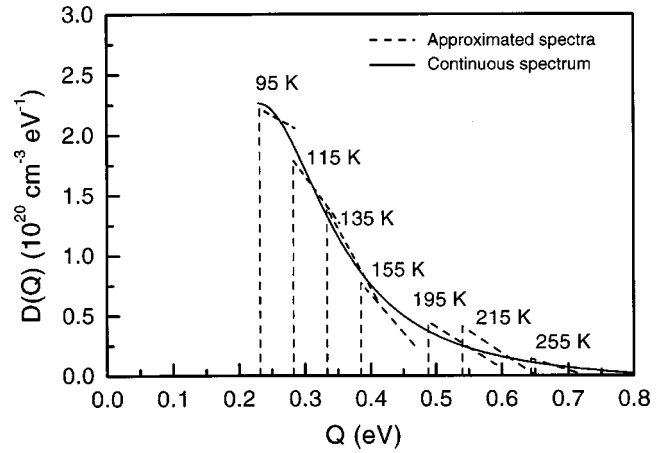


FIG. 6. The defect annihilation activation energy spectra that were calculated using Eq. (4) from the transient stress behavior after the 4 MeV Xe ion beam was switched off. Spectra are shown for seven temperatures in the range of 95–255 K (dashed lines). The drawn line is a smooth fit through the spectra, representing the defect annihilation spectrum.

ion beam is switched off, defects are annealing that have activation energies which lie in a narrow band (order kT) around

$$Q_t = kT \ln(t \cdot kT/h). \quad (6)$$

The rate at which the stress changes at time t is determined by the pre-factor, $D(Q_t)$, in Eq. (4). Vice versa, $D(Q)$ can be approximated from the measured time dependence of the stress²¹

$$D(Q_t) \cong \frac{\rho}{kT} \frac{d(\Delta\rho/\rho)}{d(\ln[t \cdot kT/h])}. \quad (7)$$

Summarizing this procedure, the defect annihilation activation spectrum, $D(Q)$, that expresses the density change associated with the annealing of defects with an activation energy Q can be approximated by taking the slope of the measured curves in Fig. 5 at each time t , where t is directly related to Q .

Figure 6 shows the activation energy spectrum, $D(Q)$, derived from the data taken at 95 K (the dashed line labeled 95 K). It was obtained by first fitting a second-order polynomial to the data in Fig. 5 and then applying Eq. (7) to calculate $D(Q)$ from the fit. As can be seen, the calculated spectrum shows a sharp increase at $Q=0.23$ eV, implying that no significant steady state concentration of defects with $Q < 0.23$ eV builds up during irradiation. The spectrum peaks at $2.2 \times 10^{20} \text{ cm}^{-3} \text{ eV}^{-1}$ and shows a gradual decrease with energy. At 95 K no data were obtained for activation energies higher than 0.29 eV since the stress measurement was halted after 720 s. Figure 6 also includes activation energy spectra obtained from measurements at other temperatures such as, e.g., shown in Fig. 5. As can be seen, a sharp cutoff is observed in all spectra, and the cutoff activation energy increases with temperature. At all temperatures the spectral density shows a decrease with temperature, and comparing all spectra measured at different temperatures, they seem to fit on one continuous spectrum that gradually decreases between 0.23 and 0.80 eV. To confirm this, a smooth curve

$D(Q)$ was fitted to the spectra of Fig. 6 (drawn line). The time dependence of the stress change was then calculated using this spectrum and Eq. (4), and the result is shown for four temperatures in Fig. 5 (dashed lines). Good agreement with the measured data is observed. The total relative volume change associated with the annihilation of defects after irradiation at 95 K can now be calculated by integrating $D(Q)$ and is found to be 0.05%.

In order to understand the observation of a continuous defect spectrum, it is important to first realize that defects are produced in a thermal spike, and hence the defect generation will be independent of the sample temperature. It may be assumed that due to the high temperature in the spike all memory of the defect population prior to the spike is “washed out.” After each ion impact the defect annihilation rate is then determined by the sample temperature and the annealing activation energy of the defect, as described by Eq. (5). Whether a (steady state) defect population builds up depends on the ion flux. For the flux of 5×10^{12} ions/cm² s used in our experiment, and assuming a typical thermal spike cross section of 20 nm², each region in the SiO₂ film is excited by an ion typically every 1 s. Therefore, defects with an annealing time shorter than 1 s will anneal out between two subsequent spikes, and will not build up a steady state population (as observed, as no stress change is found for $t < 1$ s). In contrast, defects with longer annealing times than 1 s will build up a steady state population. As this cutoff time translates into activation energy in a logarithmic way [see Eq. (6)], a sharp transition is observed in the activation energy spectra in Fig. 6. The fact that the cutoff energy depends on temperature is mostly due to the kT pre-factor in Eq. (6).

As no annealing of high-energy defects (with long annealing times) occurs in between two spikes, their density is purely determined by the defect generation in the thermal spike. This population is therefore not dependent on temperature, explaining the continuous behavior observed in Fig. 6. From this analysis we can conclude that each ion produces a collection of defects with an activation energy spectrum that is independent of the temperature. No evidence is found for the formation of defects with activation energies >0.80 eV.

Finally, we note that relaxation measurements such as in Fig. 5 have also been performed after 2 MeV Xe irradiation.²² The activation energy spectrum derived from these data was identical to that for 4 MeV irradiation in Fig. 6. We have also varied the beam flux for 2 MeV irradiation in the range of $(1-5) \times 10^{11}$ Xe/cm² s and no significant difference in the spectrum was observed.

IV. CONCLUSIONS

In situ measurements were made of the mechanical stress in thermally grown SiO₂ films on Si during 4 MeV Xe irradiation at temperatures in the range from 95 to 575 K. Four radiation-induced effects occur, that each have a characteristic effect on the stress state of the film: a structural

transformation to a state with higher equilibrium density, densification by viscous flow, anisotropic expansion, and point defect generation. The interplay between these effects is explained. The densification decreases from 3.2% to 1.7% for temperatures increasing from 95 K to 575 K. The in-plane strain generation per Xe ion decreases from $(2.5 \pm 0.4) \times 10^{-17}$ cm²/ion at 95 K to $(-0.9 \pm 0.7) \times 10^{-17}$ cm²/ion at 575 K. This decrease with temperature was confirmed by a study of the temperature dependence of the radiation-induced deformation of trenches etched in silica. The point defect activation energy spectrum peaks below 0.23 eV and then gradually decreases until it vanishes above 0.80 eV, and the relative volume change due to these defects is 0.05% at 95 K. All four irradiation-induced effects can be described using a thermal spike model.

ACKNOWLEDGMENTS

It is a pleasure to thank Joost Frenken, Pieter Kik, and Jan van der Elksen for fruitful discussions. The authors also acknowledge Koos van Uffelen for film preparation and Leo van Ijzendoorn for RBS measurements. This work is part of the research program of the “Stichting voor Fundamenteel Onderzoek der Materie (FOM),” which is financially supported by the “Nederlandse Organisatie voor Wetenschappelijke Onderzoek (NWO).”

- ¹R. A. B. Devine, Nucl. Instrum. Methods Phys. Res. B **91**, 378 (1994).
- ²W. Primak, J. Appl. Phys. **35**, 1342 (1964).
- ³C. A. Volkert and A. Polman, Mater. Res. Soc. Symp. Proc. **235**, 3 (1992).
- ⁴E. Snoeks, A. Polman, and C. A. Volkert, Appl. Phys. Lett. **65**, 2487 (1994).
- ⁵E. Snoeks, T. Weber, A. Cacciato, and A. Polman, J. Appl. Phys. **78**, 4723 (1995).
- ⁶M. L. Brongersma, E. Snoeks, and A. Polman, Appl. Phys. Lett. **71**, 1628 (1997).
- ⁷S. Klaumünzer, Changlin-Li, S. Löffler, M. Rammensee, G. Schumacher, and H. C. Neitzert, Radiat. Eff. **108**, 131 (1989).
- ⁸A. Benyagoub, S. Löffler, M. Rammensee, S. Klaumünzer, and G. Seaman-Ischenko, Nucl. Instrum. Methods Phys. Res. B **65**, 228 (1992).
- ⁹S. Klaumünzer and G. Schumacher, Phys. Rev. Lett. **51**, 1987 (1983).
- ¹⁰C. A. Volkert, J. Appl. Phys. **70**, 3521 (1991).
- ¹¹ $Y_{Si} = 181$ GPa, W. A. Brantley, J. Appl. Phys. **44**, 534 (1973).
- ¹² $Y_{Ox} = 1.0 \times 10^{11}$ Pa, H. Scholze, *Glass* (Springer, New York, 1991).
- ¹³ Y_{Ox} is known to vary by less than 5% due to irradiation, R. Brückner, J. Non-Cryst. Solids **5**, 123 (1970).
- ¹⁴Note that these stress measurements are only sensitive probes of the in-plane strain or density in the film. For a given structural configuration the out-of-plane elastic strain is related to the in-plane strain by the Poisson ratio. In addition, due to the structural transformation, the out-of-plane density will decrease.
- ¹⁵F. F. Morehead, Jr. and B. L. Crowder, Radiat. Eff. **6**, 27 (1970).
- ¹⁶H. Trinkaus and A. I. Ryazanov, Phys. Rev. Lett. **74**, 5072 (1995).
- ¹⁷ $\nu = 0.17$, $\alpha = 5 \times 10^{-7}$ K⁻¹, $\rho = 2.2 \times 10^3$ kg/m³, $C = 1.25$ kJ/mol K, H. Scholze, in Ref. 12.
- ¹⁸ $S = 5 \times 10^{-7}$ J/m, calculated using TRIM, a Monte Carlo simulation program, J. F. Ziegler, J. P. Biersack, and U. Littmark, *The Stopping and Range of Ions in Solids* (Pergamon, New York, 1985).
- ¹⁹A. I. Ryazanov, A. E. Volkov, and S. Klaumünzer, Phys. Rev. B **51**, 12107 (1995).
- ²⁰T. van Dillen, M. L. Brongersma, E. Snoeks, and A. Polman, Nucl. Instrum. Methods Phys. Res. B **148**, 221 (1999).
- ²¹W. Primak, Phys. Rev. **100**, 1677 (1955).
- ²²T. van Dillen, Masters thesis, Utrecht University (FOM-Institute for Atomic and Molecular Physics, Amsterdam, 1999).